Dependence of angle-resolved photoemission spectra of high-temperature superconductors on the spin-fluctuation susceptibility

L. Coffey, D. Lacy, K. Kouznetsov,* and A. Erner†
Department of Physics, Illinois Institute of Technology, Chicago, Illinois 60616
(Received 20 February 1997)

Angle-resolved photoemission-spectroscopy (ARPES) measurements on high-temperature superconductors, such as Bi-Sr-Ca-Cu-O, show three main components: these are a quasiparticle spectral peak that develops below the superconducting transition temperature T_c, an accompanying broad background of secondary electrons, and a dip feature beside the main quasiparticle peak. The broad background may originate from inelastic processes in which the photoelectron emits and absorbs spin fluctuations. Calculations of the quasiparticle spectral weight are presented incorporating these spin-fluctuation-mediated inelastic processes in which the development of the superconducting gap Δ has been incorporated into the magnetic susceptibility $\chi(\mathbf{q},E)$. A dip feature develops below T_c in the quasiparticle spectral weight due to the shifting of spin-fluctuation spectral weight, $\mathrm{Im}\chi(\mathbf{q},E)$, from low energies to energies greater than 2Δ. These results provide evidence that the dip feature in the ARPES spectrum in high-temperature superconductors such as Bi-Sr-Ca-Cu-O is an opening of a spin gap below T_c. [S0163-1829(97)05933-X]

INTRODUCTION

Angle-resolved photoemission spectroscopy (ARPES) has developed into an important probe of the superconducting and normal-state properties of the cuprate-oxide, high-temperature superconductors. ARPES measurements support local-density approximation predictions for the electronic band structure of the cuprates[1] and a $d_{x^2-y^2}$ symmetry superconducting order parameter.[2] ARPES provides information on how this gap evolves with doping and its connection to the normal-state gap seen in underdoped cuprates.[3]

The overall shape of the ARPES spectra measured in these experiments is not fully understood, however. A common feature of the data is the coexistence of a broad background and a peak. The latter is interpreted as the quasiparticle spectral weight peak of the Fermi surface electrons emitted from the crystal after the absorption of the ultraviolet photon ($\simeq 20$ eV). The relative heights of the background and the peak vary from one experiment to another.[2,4,5] In addition to the background, a dip feature is seen to develop when the crystal is cooled below the superconducting transition temperature.[2] The connection between this dip feature and a similar feature observed in tunneling experiments on the cuprates[6–8] has been the subject of recent investigations by the present authors.[9,10] The tunneling density of states is another measure of the quasiparticle spectral weight. The difference between tunneling and ARPES arises, in part, because tunneling measurements provide an average of the quasiparticle spectral weight along a line of states in the Brillouin zone, determined by the directional tunneling matrix element.[10] ARPES measurements provide information about the quasiparticle spectral weight in a small region, determined by experimental resolution, around a **k**-space point on the Fermi surface.

Recent work[10] proposed a common explanation for the broad ARPES background and the linearly increasing tunneling conductances seen in many high-temperature superconductor tunnel junctions.[11] It was proposed that the ARPES background is due to the simultaneous emission or absorption of spin fluctuations by the electron as it is escapes from the surface layer of the crystal after absorbing the ultraviolet photon. The same processes can occur in the surface layer near the tunnel barrier in a tunnel junction and can lead to a wide variety of tunneling conductances. Related work has been carried out by others.[12,13]

Previous work[10] made use of a phenomenological model for the spin-fluctuation spectral weight which had been used to fit inelastic neutron-scattering measurements of the spin-fluctuation spectrum in Y-Ba-Cu-O.[14] This model for the spin-fluctuation spectrum did not have superconducting correlations incorporated in it. This issue has become relevant due to the observation of structure in the spin-fluctuation spectrum which appears to be directly connected to the development of superconductivity in the cuprates.[15] Another important issue is the relative height of the main spectral peak and the background as well as its dependence on the underlying magnitude of the spin-fluctuation susceptibility. The overall magnitude of the inelastic background contribution to the quasiparticle spectral weight was multiplied by a constant fitting factor in Ref. 10 in order to reproduce results that compare favorably with ARPES data.

In the present work, the spin-fluctuation spectral weight, $D(E)$, which determines the inelastic background, is calculated using the random-phase approximation (RPA) for the underlying electronic spin susceptibility, $\chi(\mathbf{q},E)$. The present calculations incorporate the tight-binding band structure with next-nearest-neighbor hopping, appropriate for materials of interest such as Bi-Sr-Ca-Cu-O, and superconductivity arising from a $d_{x^2-y^2}$ symmetry order parameter. The effects of the superconducting state on the spin-fluctuation spectrum are incorporated into a calculation of $A(\mathbf{k},E)$ and a comparison is made between predictions and experimental ARPES measurements of $A(\mathbf{k},E)$ above and below T_c.

One of the results of this work is the prediction that the dip feature seen in ARPES data below T_c on Bi-Sr-Ca-Cu-O (Ref. 2) is indirect evidence of the development of the spin gap in $\chi(\mathbf{q},E)$ due to the onset of superconductivity. The present work allows a controlled investigation to be carried

out of the dependence of the relative magnitude of the inelastic background and the main quasiparticle peak on the strength of the electron-spin fluctuations. Finally, the Van Hove peak in the underlying tight band structure which can strongly influence the energy dependence of the spin-fluctuation spectral weight $D(E)$, is included.

The present model for the quasiparticle spectral weight $A(\mathbf{k},E)$ assumes that the main peak in the ARPES spectrum arises from photoelectrons created by the absorption of ultraviolet photons by electrons at the Fermi energy. The accompanying broad background is due to the simultaneous absorption or emission of spin fluctuations by other electrons as they absorb photons. Spin-fluctuation emission dominates at the low temperatures of interest here. In the ARPES experimental technique, the momentum or **k**-space region being probed can be identified with relatively good precision using energy and momentum conservation. The photoelectrons which contribute to the inelastic background are secondary electrons, which having emitted spin fluctuations, are scattered into the same momentum direction **k**, as those electrons which yield the main ARPES spectral peak. They are collected by the detector and labeled with the same momentum **k** as the main peak yielding an overall APRES spectrum for a particular **k** vector.

THEORETICAL MODEL

The total quasiparticle spectral weight, $A(\mathbf{k},E)$, in our model is made up of two contributions. The main peak is calculated from

$$A^0(\mathbf{k},E)=-\frac{1}{\pi}\,\mathrm{Im}G(\mathbf{k},E), \tag{1}$$

where

$$G(\mathbf{k},E)=\frac{E+i\Gamma+\xi_k}{(E+i\Gamma)^2-\xi_k^2-\Delta_k^2}. \tag{2}$$

The electronic band structure is defined as

$$\xi_k=-2t[\cos(k_x)+\cos(k_y)]-4t'\,\cos(k_x)\cos(k_y)-\mu$$

where we have chosen a typical value for the cuprates of $t'=-0.45t$. The superconducting order parameter is given by $\Delta_k=\Delta_0[\cos(k_x)-\cos(k_y)]/2$ with $\Delta_0=0.1t$. An electronic damping parameter is also included through $\Gamma=\Gamma_0+\Gamma_1(T/T_c)^3$ with Γ_0 and Γ_1 chosen to be $0.04t$ and $0.05t$, respectively. The chemical potential μ is chosen to be $-1.75t$.

The inelastic contribution is calculated from

$$\begin{aligned}A_{\mathrm{inel}}(\mathbf{k},E)=-\frac{1}{\pi}\int_{-\infty}^{+\infty}dE'\;\mathrm{Im}G(\mathbf{k},E')\{&D(E-E')\\&\times[n(E-E')+f(-E')]\Theta(E-E')\\&+D(E'-E)\\&\times[n(E'-E)+f(E')]\Theta(E'-E)\},\end{aligned} \tag{3}$$

where $n(E)$ denotes the Bose-Einstein distribution and $f(E)$ denotes the Fermi function.

The spin-fluctuation spectral weight $D(E)$ is defined as the momentum-integrated spin-fluctuation susceptibility multiplied by the square of the electron-spin fluctuation coupling constant g/t,

$$D(E)=\frac{1}{(2\pi)^2}\int_{-\pi}^{+\pi}dq_x\int_{-\pi}^{+\pi}dq_y(g/t)^2\;\mathrm{Im}\chi(\mathbf{q},E), \tag{4}$$

where

$$\mathrm{Im}\chi(\mathbf{q},E)=\frac{\mathrm{Im}\chi^0(\mathbf{q},E)}{\{[1-g\;\mathrm{Re}\chi^0(\mathbf{q},E)]^2+[g\;\mathrm{Im}\chi^0(\mathbf{q},E)]^2\}}. \tag{5}$$

The imaginary part of the bare electronic spin susceptibility is defined as

$$\begin{aligned}\mathrm{Im}\chi^0(\mathbf{q},E)=\Sigma_{\mathbf{p}}\int_{-\infty}^{+\infty}dE'[f(E'+E)-f(E')]\{&[(u_{p+q}^2u_p^2+u_pv_pu_{p+q}v_{p+q})]\mathrm{Im}G(p+q,E'+E)\mathrm{Im}G(p,E')\\&+[u_{p+q}^2v_p^2-u_pv_pu_{p+q}v_{p+q}]\mathrm{Im}G(p+q,E'+E)\mathrm{Im}G(p,-E')+[v_{p+q}^2u_p^2-u_pv_pu_{p+q}v_{p+q}]\\&\times\mathrm{Im}G(p+q,-E'-E)\mathrm{Im}G(p,E')+[v_{p+q}^2v_p^2+u_pv_pu_{p+q}v_{p+q}]\mathrm{Im}G(p+q,-E'-E)\mathrm{Im}G(p,-E')\},\end{aligned} \tag{6}$$

where u_p and v_p represent the usual superconducting coherence factors and

$$\mathrm{Im}G(p,E)=\frac{1}{\pi}\,\frac{\Gamma}{(E-E_p)^2+\Gamma^2}, \tag{7}$$

where $E_p=\sqrt{(\xi_p^2+\Delta_p^2)}$. The real part of $\chi^0(\mathbf{q},E)$ is obtained by Kramers-Kronig transform.

The total quasiparticle spectral weight is then given by

$$A(\mathbf{k},E)=A^0(\mathbf{k},E)+\alpha A_{\mathrm{inel}}(\mathbf{k},E), \tag{8}$$

where α is an overall constant multiplicative factor which determines the relative contributions of the elastic $A^0(\mathbf{k},E)$ channel and the inelastic channel $A_{\mathrm{inel}}(\mathbf{k},E)$. For the results presented in this paper, α is chosen to be in the range from 1 to 4, depending on the values chosen for the other physical parameters in the calculation of $A(\mathbf{k},E)$. The choice of α incorporates the relative weighting of the bulk [leading to $A^0(\mathbf{k},E)$] and surface physics [leading to $A_{\mathrm{inel}}(\mathbf{k},E)$].

In our previous[10] work based on Ref. 16, the expression for the total spectral weight of Eqs. (3) and (8) was extracted from the expression for the total elastic and inelastic tunneling current which can be written as

$$I(V)=\int dE N_S(E)N_N(E-eV)[f(E)-f(E-eV)], \quad (9)$$

where

$$N_S(E)=\Sigma_{\mathbf{k}}|T_k^{\mathrm{el}}|^2[A_0(\mathbf{k},E)+\alpha A_{\mathrm{inel}}(\mathbf{k},E)]. \quad (10)$$

In obtaining Eqs. (3) and (8), the tunneling matrix element squared in the inelastic contribution to the current, $I(V)$, denoted by $|\Lambda^{(1,1)}|^2$ in Eq. (19.37b) of Ref. 16, was assumed to be given by $|\Lambda^{(1,1)}|^2=\alpha|\Lambda^{(1,0)}|^2(g/t)^2$. By replacing ϵ_L with ϵ_L-eV in Eqs. (19.33b) and (19.37c) of Ref. 16, the combined elastic and inelastic current can then be written as in Eq. (9) (using the notation $|T_k^{\mathrm{el}}|^2$ in place of $|\Lambda^{(1,0)}|^2$). The spectral weight function of Eq. (8) yields the density of states $N_S(E)$ using Eq. (10).

The inelastic tunneling channel described here implies that an electron tunnels into the superconducting crystal along a direction determined by the directional tunneling matrix element T_k^{el} and then emits a spin fluctuation which brings in the spin-fluctuation coupling constant g/t into the overall tunneling matrix element. The spectral weight function of Eq. (8), which determines the density of states in Eq. (10), can then be used to interpret ARPES data.

One approximation in the present approach is the lack of conservation of momentum. This approximation is also a feature of related work in this field.[12,13] This approximation is valid for the case of sufficiently high electronic disorder and scattering which will broaden the underlying $A^0(\mathbf{k},E)$. In the clean limit, Eq. (3) should contain terms involving $\Sigma_{\mathbf{q}}\,\mathrm{Im}G(\mathbf{k}+\mathbf{q},E')\mathrm{Im}\chi(\mathbf{q},E-E')$ within the integral on the right-hand side of the equation which would require a significant increase in numerical computation to yield an accurate answer for $A_{\mathrm{inel}}(\mathbf{k},E)$. The assumption inherent in the present work is that $\mathrm{Im}G(\mathbf{k}+\mathbf{q},E')$ is sufficiently broadened by disorder that it is a reasonable approximation to take it outside the sum over spin-fluctuation wave vectors $\mathbf{q}$ and replace it with $\mathrm{Im}G(\mathbf{k},E')$. This approximation can also be further justified by noting that $\mathrm{Im}\chi(\mathbf{q},E-E')$ is strongly peaked at $\mathbf{Q}=(\pi,\pi)$ and that for the electronic wave vectors of interest here $\mathrm{Im}G(\mathbf{k},E')\simeq\mathrm{Im}G(\mathbf{k}+\mathbf{Q},E')$. We have also tested that the results for the total quasiparticle spectral weight to be presented in the accompanying figures can be generated with higher values of damping Γ, and correspondingly more broadened $A^0(\mathbf{k},E)$, than have been used in the work shown here.

RESULTS

Figures 1 and 2 show results for the spin-fluctuation spectral weight $D(E)$ for the case of a constant coupling constant $g=U$. Figure 1 depicts $D(E)t$ at $T/T_c=1.0$ and 0.3. The effect of the onset of superconductivity is evident in the figure in the removal of spectral weight from below $2\Delta_0$ to higher energies.

In the figures depicting $D(E)t$ in the present work, the underlying value of $\Sigma_{\mathbf{q}}\mathrm{Im}\chi(\mathbf{q},E)$ is given by dividing $D(E)t$ by $(U/t)^2$. For example, the peak value for $D(E)t$ of approximately 0.3 in Fig. 1 implies an underlying value of $\Sigma_q\,\mathrm{Im}\chi(q,E)$ of 2.0 states per eV assuming a value of $t=150$ meV.

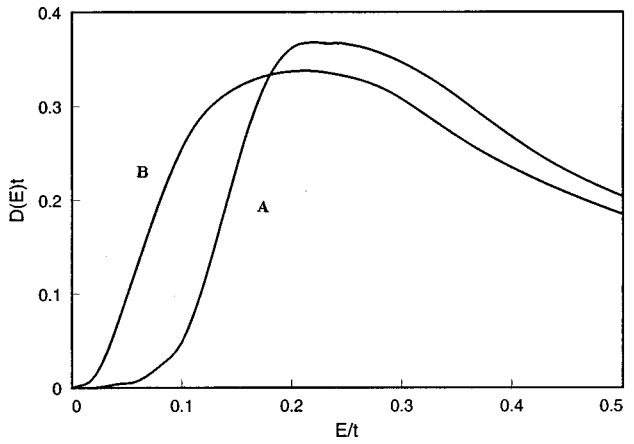

FIG. 1. The momentum integrated spin-fluctuation spectral weight $D(E)t$ from Eq. (4) for $g=U=1.0t$. Curve A is for $T/T_c=1.0$ and curve B is for $T/T_c=0.3$.

In calculating the two curves in Fig. 1, the sum rule

$$\frac{1}{2\pi^2}\int d^2q\int_{-\infty}^{+\infty}dE\,\frac{\mathrm{Im}\chi(q,E)}{[1-\exp(-E/k_BT)]}=\mathrm{const} \quad (11)$$

is imposed. The same value of $U=1.0t$ was used for the two $D(E)$ curves in Fig. 1 with $\mu=-1.75t$. Figure 2 depicts $D(E)t$ for the case $U=1.5t$ which is close to the largest possible value of U/t for the choice of $\mu=-1.75t$ before the RPA approximation for $\chi(q,E)$ breaks down.

The resulting quasiparticle spectral weight curves, $A(\mathbf{k},E)t$, for these $D(E)t$ curves are depicted in Figs. 3, 4, and 5. All $A(\mathbf{k},E)t$ curves presented in this paper are calculated for $\mathbf{k}$ on the Fermi surface at $\mathbf{k}=(\pi,0.1624)$. Figure 3 depicts $A(\mathbf{k},E)t$ for the $D(E)t$ of Fig. 1, with $\alpha=4.0$ in Eq. (8). The development of the dip feature associated with the onset of the spin-gap in $D(E)t$ is clearly visible below the superconducting transition temperature.

Figures 4 and 5 depict $A(\mathbf{k},E)t$ using the $D(E)t$ of Fig. 2 and use $\alpha=1$ for Fig. 4 and $\alpha=1.5$ for Fig. 5. The large

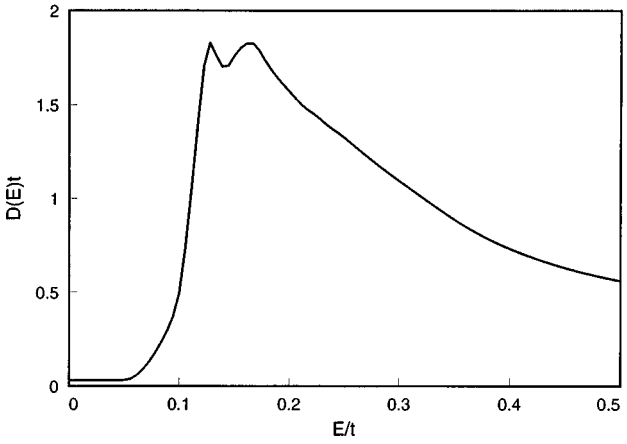

FIG. 2. The momentum integrated spin-fluctuation spectral weight $D(E)t$ from Eq. (4) for $g=U=1.5t$ for $T/T_c=0.3$.

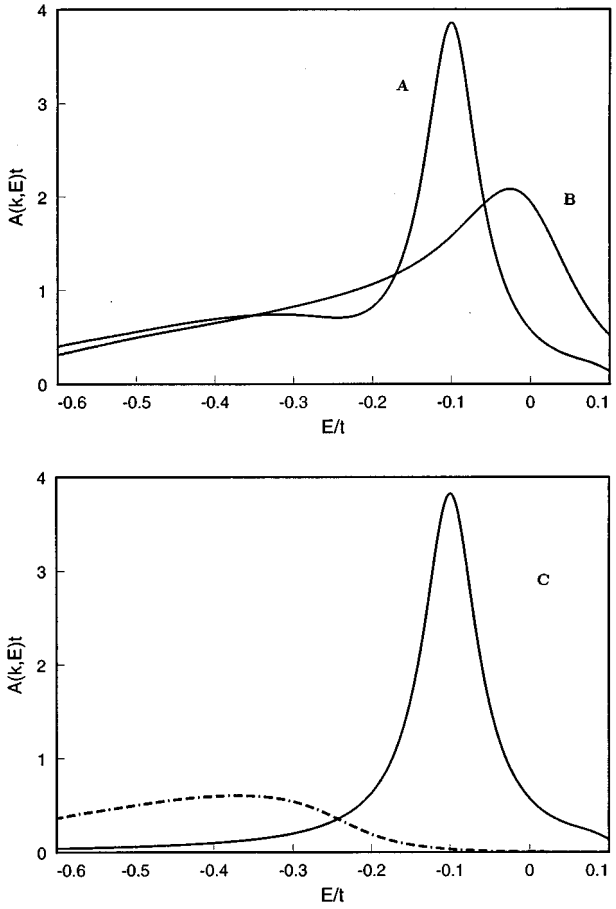

FIG. 3. (Top): The quasiparticle spectral weight $A(\mathbf{k},E)t$ for $\mathbf{k}$ on the Fermi surface. α of Eq. (8) is 4.0. This curve is generated using $D(E)t$ of Fig. 1. $\mathbf{k}$ is chosen to be $(\pi, 0.1624)$ on the Fermi surface. Curve A is for $T/T_c=0.3$ and curve B is for $T/T_c=1.0$. (Bottom): Curve C depicts the contributions of the elastic and inelastic channels separately for $T/T_c=0.3$. The contributions of the two channels depicted in curve C are typical of the other $A(\mathbf{k},E)t$ curves in this paper.

increase in magnitude of $D(E)t$ in Fig. 2 compared to that of Fig. 1 allows a sizeable inelastic background to occur from Eq. (8) with the elastic and inelastic channels contributing about equally. Unlike Ref. 10, the connection between α and

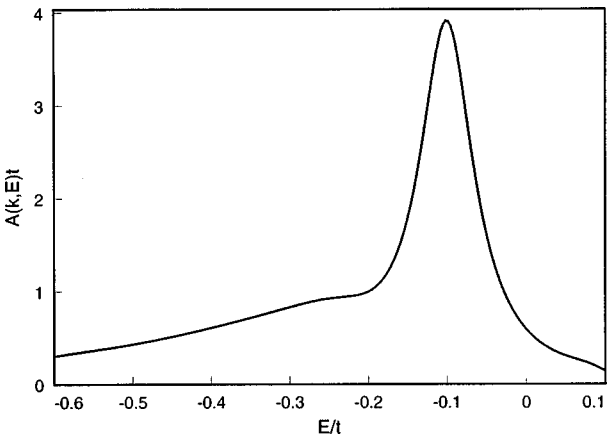

FIG. 4. The quasiparticle spectral weight $A(\mathbf{k},E)t$ for $\mathbf{k}$ on the Fermi surface. α of Eq. (8) is 1.0. This curve is generated using $D(E)t$ of Fig. 2. $\mathbf{k}$ is chosen to be $(\pi, 0.1624)$ on the Fermi surface.

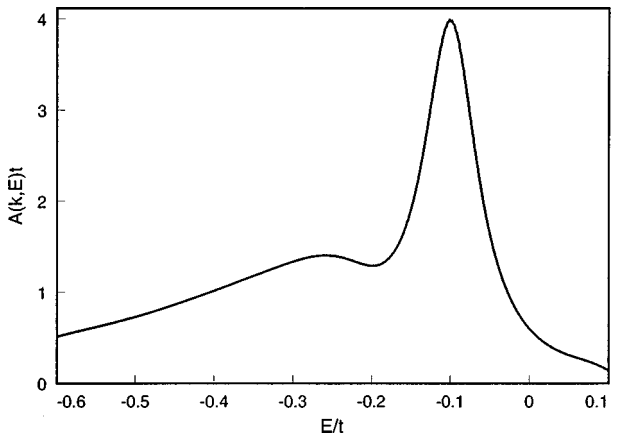

FIG. 5. The quasiparticle spectral weight $A(\mathbf{k},E)t$ for $\mathbf{k}$ on the Fermi surface. α of Eq. (8) is 1.5. This curve is generated using $D(E)t$ of Fig. 2. $\mathbf{k}$ is chosen to be $(\pi, 0.1624)$ on the Fermi surface.

the magnitude of the underlying $\mathrm{Im}\chi(q,E)$, which is determined by U/t from Eq. (5) can now be explored in a controlled manner. The effect of interactions in $D(E)t$ is to shift the peak slightly below $2\Delta_0$ as can be seen by comparing $D(E)$ in Figs. 1 and 2. This effect can result in a disappearance of the dip feature in $A(\mathbf{k},E)t$ as can be seen in Fig. 4. However, a slight increase in α restores the feature as shown in Fig. 5. Figure 6 is generated using the $D(E)t$ of Fig. 2 with $\alpha=3.0$, $\Gamma_0=0.06t$, and $\Gamma_1=0.075t$ in Eq. (2). These figures illustrate the wide variation in the relative heights of the main elastic peak and inelastic background in $A(\mathbf{k},E)t$ that can be generated within the present model. A similar variation is seen in ARPES experiments suggesting that the background is not a bulk phenomenon but instead a reflection of the surface physics which can probably vary from sample to sample.

The peak at $E=2\Delta_0$ in $D(E)t$ in Figs. 1 and 2 is caused by a strong peak in the underlying $\mathrm{Im}\chi(q,E)$ at $\mathbf{q}=(\pi,\pi)$ at $E=2\Delta_0$ for $\mu=-1.75t$. This peak shifts downwards in E as U increases due to the part of the denominator involving $\mathrm{Re}\chi(q,E)$ in Eq. (5) for the susceptibility. As has been just pointed out, the extent to which this occurs can influence the

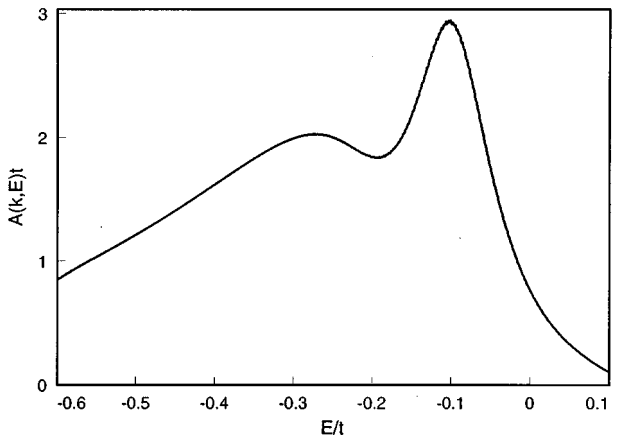

FIG. 6. The quasiparticle spectral weight $A(\mathbf{k},E)t$ for $\mathbf{k}$ on the Fermi surface. α of Eq. (8) is 3.0. This curve is generated using $D(E)t$ of Fig. 2. $\Gamma_0=0.06t$ and $\Gamma_1=0.075t$ in Eq. (2). $\mathbf{k}$ is chosen to be $(\pi, 0.1624)$ on the Fermi surface.

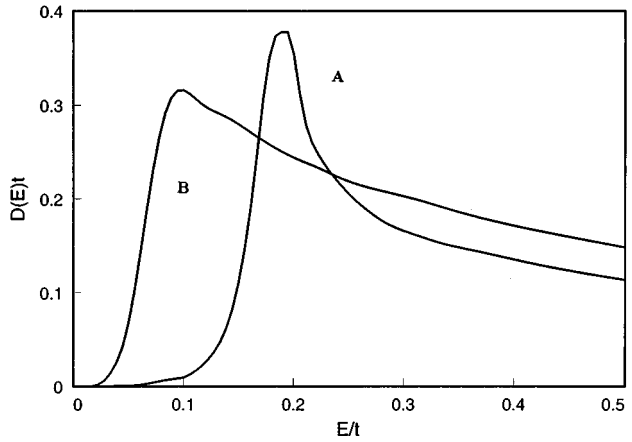

FIG. 7. The momentum integrated spin-fluctuation spectral weight $D(E)t$ from Eq. (4) for $g=J_q=-J_0[\cos(q_x+\cos(q_y)]$. Curve A is for $T/T_c=0.3$, $J_0=1.0t$ and curve B is for $T/T_c=1.0$, $J_0=1.2t$.

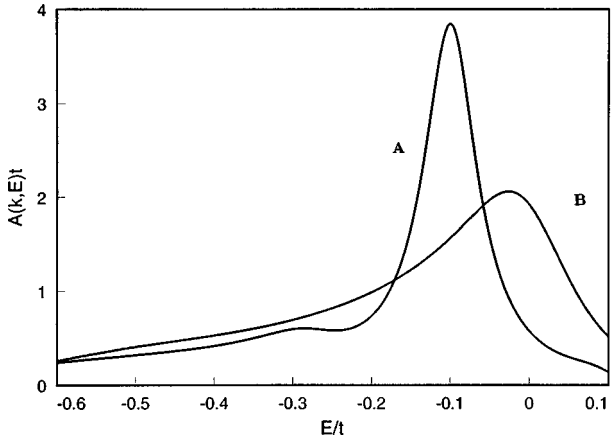

FIG. 9. The quasiparticle spectral weight $A(\mathbf{k},E)t$ for $\mathbf{k}$ on the Fermi surface. α of Eq. (8) is 4.0. This curve is generated using $D(E)t$ of Fig. 7. $\mathbf{k}$ is chosen to be $(\pi, 0.1624)$ on the Fermi surface. Curve A is for $T/T_c=0.3$ and curve B is for $T/T_c=1.0$.

ability to produce a dip feature in the spectral weight. The peak at $E=2\Delta_0$ is also sensitive to the choice of chemical potential μ. A slightly smaller negative value for μ will result in the peak moving to higher energies in $\mathrm{Im}\chi(q,E)$ and diminishing in height.[17] The $E=2\Delta_0$ peak in $\mathrm{Im}\chi(q,E)$ is the result of the underlying Van Hove peak in the tight-binding band structure and moves to different values of E as the chemical potential is varied.

Figures 7 and 8 depict $D(E)t$ for the choice $g=-J_0[\cos(k_x)+\cos(k_y)]$,[18] which enhances the role of the (π,π) peak in $\mathrm{Im}\chi(q,E)$. $J_0=1.0t$ and $1.2t$ for Figs. 7A and 7B and $J_0=1.2t$ and $1.4t$ for Figs. 8A and 8B. This choice of values for J_0 ensures that the sum rule of Eq. (11) is satisfied.[19] The resulting $A(k,E)t$ are depicted in Figs. 9 [which uses the $D(E)t$ of Figs. 7] and 10 [which uses the $D(E)t$ of Fig. 8] for $\alpha=4.0$ and $\alpha=2.0$, respectively. In calculating $A_{\mathrm{inel}}(\mathbf{k},E)t$ from Eq. (3), the spectral weight $D(E)t$ is integrated over energy E' and, as a result, sharp peak structure in $D(E)t$ is somewhat smeared out in the resulting $A(k,E)t$.

The effect on $A(\mathbf{k},E)t$ of choosing a different point in $\mathbf{k}$ space has been investigated before in Ref. 10. Anisotropy as a function of $\mathbf{k}$ enters into the calculation of the quasiparticle spectral weight in several ways. Apart from the underlying electronic band structure ξ_k, the most significant sources of anisotropy are in the order parameter Δ_k and in strong coupling effects such as the quasiparticle damping rate, Γ. This last issue was treated phenomenologically in Ref. 10 by increasing the value of Γ for those regions of $\mathbf{k}$ space where $\Delta_k=0$. The overall effect is to smear out the main quasiparticle peak and, as a result, eliminate the dip feature in the quasiparticle spectral weight.

The spin-fluctuation spectral weight $D(E)t$ can also be used to estimate the quasiparticle damping rate, denoted by Γ in Eq. (2), from

$$\Gamma=2\pi\int_0^{E_{\max}}dE\,\frac{D(E)t}{\sinh(E/k_BT)}. \tag{12}$$

Using the $D(E)t$ from Fig. 1B for $T/T_c=1$ and assuming $\Delta_0=2k_BT_c$, Γ is found to be $0.06t$. This value is comparable to values of the quasiparticle damping rate Γ used in generating the results of Figs. 1–10.

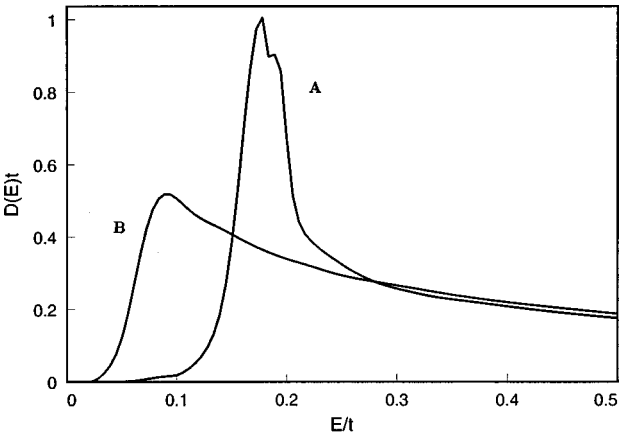

FIG. 8. The momentum-integrated spin-fluctuation spectral weight $D(E)t$ from Eq. (4) for $g=J_q=-J_0[\cos(q_x+\cos(q_y)]$. Curve A is for $T/T_c=0.3$, $J_0=1.2t$ and curve B is for $T/T_c=1.0$, $J_0=1.4t$.

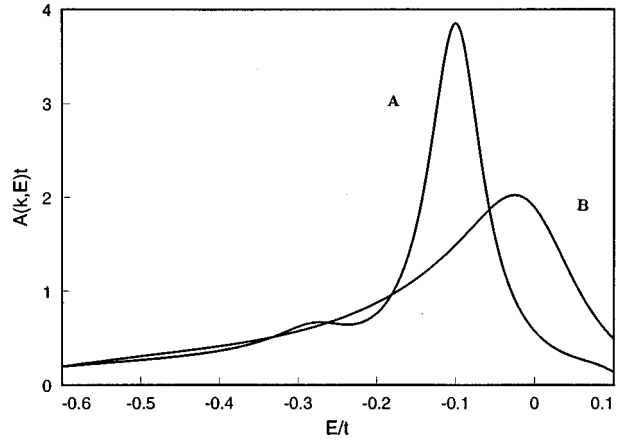

FIG. 10. The quasiparticle spectral weight $A(\mathbf{k},E)t$ for $\mathbf{k}$ on the Fermi surface. α of Eq. (8) is 2.0. This curve is generated using $D(E)t$ of Fig. 8. $\mathbf{k}$ is chosen to be $(\pi, 0.1624)$ on the Fermi surface. Curve A is for $T/T_c=0.3$ and curve B is for $T/T_c=1.0$.

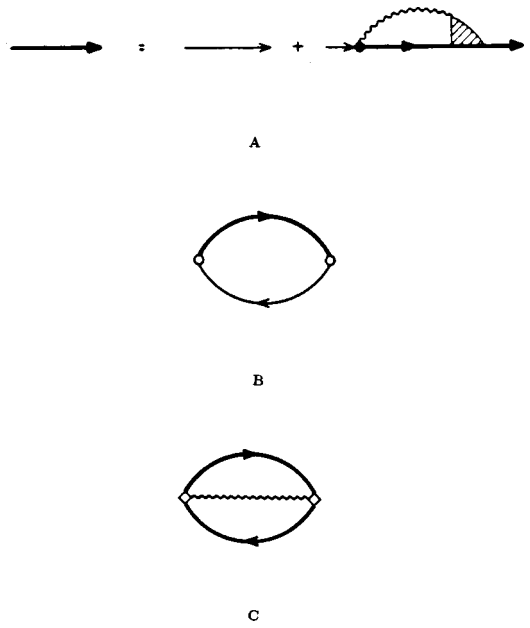

FIG. 11. *A* and *B* depict conventional strong-coupling corrections to the electron Greens function and the corresponding diagram for calculating the tunneling current. *C* depicts the diagram describing inelastic tunneling. The wavy lines represent spin fluctuations in the figures.

Equation (12) is derived from the conventional strong-coupling treatment of spin fluctuations. The model for the contribution of the inelastic background in this paper is different from conventional treatments of strong-coupling effects in calculations of the quasiparticle spectral weight and tunneling densities of states. The role of spin fluctuations in the cuprates has been widely investigated in both the normal and superconducting states.[20–22] The resulting quasiparticle spectral weights $A(\mathbf{k},E)$ in these calculations can be used to generate density of states curves from $N(E) = \Sigma_k |T_k|^2 A(\mathbf{k},E)$. In the superconducting state, densities of states curves will display small corrections relative to the underlying weak-coupling densities of states. This will not provide an explanation for the rapidly increasing tunneling densities of states at high bias voltages measured in tunneling experiments on the cuprates.[11] This type of variation with bias voltage is a signature of an additional inelastic channel, which in the cuprates is assumed to involve the emission and absorption of spin fluctuations in the surface region of the sample.

The difference between the inelastic tunneling model and conventional strong-coupling approaches can also be seen by considering the type of Feynman diagrams that arise in the usual calculation of the tunneling current using linear-response theory. These are shown in Fig. 11. Conventional strong-coupling corrections are incorporated with diagrams of the type shown in Fig. 103 combined with Fig. 100(a) of Ref. 16, shown in Figs. 11(A) and 11(B). Inelastic tunneling is calculated using a different diagram as depicted in Fig. 98 of Ref. 16, shown in Fig. 11(C), where both vertices of the diagram are joined by the propagator representing the spin fluctuation.

CONCLUSIONS

The spin gap below $E = 2\Delta_0$ in Im $\chi(q,E)$ in Figs. 1, 2, 7, and 8 occurs because a spin fluctuation must have an energy E greater than or equal to this threshold in order to create a quasiparticle-quasihole pair at low temperatures. The effects of this on the quasiparticle spectral weight and tunneling density of states has been investigated before in different ways.[23,24] Littlewood and Varma incorporated this type of pair-breaking physics phenomenologically in a model based on the marginal Fermi-liquid theory for *s*-wave superconductivity and investigated the resulting quasiparticle spectral weight and density of states curves. In Ref. 24, a quasiparticle damping mechanism based on the same pair-breaking mechanism for *a* $d_{x^2-y^2}$ order parameter was incorporated approximately into the quasiparticle spectral weight and the resulting superconductor-insulator-superconductor current characteristics were calculated for comparison with experiment.[7]

The work of Ref. 10, which is the basis for the present calculations, used a phenomenological model for the spin-fluctuation spectral weight. In Ref. 10, a dip feature is present in the quasiparticle spectral weight due to a combination of the narrowing of the main peak, because of the reduction of the scattering rate in the superconducting state, and the underlying shape of the model used for Im$\chi(q,E)$. No superconducting correlations were incorporated into the model for $\chi(q,E)$ which are now known to be important[15] and the dip feature was an accidental feature of the model.

In conclusion, results for a model of the quasiparticle spectral weight $A(\mathbf{k},E)t$ have been presented which incorporate a conventional elastic peak and an inelastic background arising from spin-fluctuation emission processes; Eq. (3). The goal is to interpret ARPES measurements on high-temperature superconductors. The results of the present work provide a model connecting a microscopic calculation of the spin-fluctuation susceptibility $\chi(q,E)$, Eqs. (5) and (6), to the magnitude and overall shape of the inelastic background seen in ARPES. The spectral weight curves generated in this approach can also be used to interpret tunneling conductance measurements on high-temperature superconductors.[10] The dip feature seen in some ARPES data is caused by the development of a spin gap in the underlying spin susceptibility at the onset of superconductivity.

ACKNOWLEDGMENT

The authors acknowledge conversations with John Zasadzinski.

*Present address: Dept. of Physics, University of California, Berkeley, CA.

†Present address: Dept. of Physics, Northwestern University, Evanston, IL.

[1] S. Massida, J. Yu, and A. J. Freeman, Physica C **152**, 251 (1988).

[2] Z. X. Shen *et al.*, Phys. Rev. Lett. **70**, 1553 (1993).

[3] D. S. Marshall *et al.*, Phys. Rev. Lett. **76**, 4841 (1996).

[4] Y. Hwu *et al.*, Phys. Rev. Lett. **67**, 2573 (1991).

[5] M. Randeria *et al.*, Phys. Rev. Lett. **74**, 4951 (1995).

[6] Q. Huang, J. F. Zasadzinski, K. E. Gray, E. D. Bukowski, and D.

M. Ginsberg, Physica C **161**, 141 (1989).
[7] D. Coffey, J. Phys. Chem. Solids **54**, 1369 (1993).
[8] Ch. Renner and O. Fischer, Phys. Rev. B **51**, 9208 (1996).
[9] L. Coffey and D. Coffey, Phys. Rev. B **48**, 4184 (1993).
[10] K. Kouznetsov and L. Coffey, Phys. Rev. B **54**, 3617 (1996).
[11] For a review, see J. Zasadzinski *et al.*, in *Spectroscopic Studies of High T_c Cuprates*, edited by I. Bozovic and D. van der Marel (SPIE, Bellingham, 1996).
[12] Ming-wen Xiao and Zheng-zhong Li, Phys. Rev. B **49**, 13 160 (1994).
[13] J. Kirtley and D. J. Scalapino, Phys. Rev. Lett. **65**, 798 (1990).
[14] J. M. Tranquada *et al.*, Phys. Rev. Lett. **64**, 800 (1990).
[15] Hung Fai Fong *et al.*, Phys. Rev. Lett. **75**, 316 (1995).
[16] C. B. Duke, *Solid State Physics: Advances in Research and Applications* (Academic, New York, 1969), Suppl. 10, Sec. 19 and Eq. 19.37(c).
[17] I. I. Mazin and V. M. Yakovenko, Phys. Rev. Lett. **75**, 4134 (1995).
[18] G. Stemmann *et al.*, Phys. Rev. B **50**, 4075 (1994); D. Z. Ziu, Y. Zha, and K. Levin, Phys. Rev. Lett. **75**, 4130 (1995); J. M. Rendell and J. P. Carbotte, Phys. Rev. B **53**, 8698 (1996).
[19] The suggestion to vary J_0 with temperature in order to satisfy the sum rule of Eq. (11) is due to Y. M. Vilk. See also Y. M. Vilk, Europhys. Lett. **33**, 159 (1996).
[20] A. Kampf and J. R. Schrieffer, Phys. Rev. B **42**, 7967 (1990).
[21] P. Monthoux and D. Pines, Phys. Rev. Lett. **69**, 961 (1992).
[22] P. Monthoux and D. J. Scalapino, Phys. Rev. Lett. **72**, 1874 (1994).
[23] P. Littlewood and C. Varma, Phys. Rev. B **46**, 405 (1992).
[24] D. Coffey and L. Coffey, Phys. Rev. Lett. **70**, 1529 (1993).